Journal of Scientific Research & Reports
12(1): 1-20, 2016; Article no.JSRR.28108
ISSN: 2320-0227

SCIENCEDOMAIN *international*
www.sciencedomain.org

Image Information Measures for Predicting Image Registration Performance on iThemba LABS Image Registration System

Adebayo A. Adeleke[1*]

[1]*Department of Physics and Engineering Physics, University of Saskatchewan, Saskatoon, Canada.*

Author's contribution

The sole author designed, analyzed and interpreted and prepared the manuscript.

Article Information

DOI: 10.9734/JSRR/2016/28108
Editor(s):
(1) José Alberto Duarte Moller, Center for Advanced Materials Research, Complejo Industrial Chihuahua, Mexico.
Reviewers:
(1) Anuj Kumar Goel, Maharishi Markandeshwar University, India.
(2) R. Gayathri, Sri Venkateswara College of Engineering, India.
(3) Anonymous, Universiti Sains Malaysia, Malaysia.
Complete Peer review History: http://www.sciencedomain.org/review-history/16066

Original Research Article

Received 1st July 2016
Accepted 28th August 2016
Published 6th September 2016

ABSTRACT

Image information measures such as mutual information and entropy quotient can do more than just giving a quantitative impression on how good an image is. In recent times, they have found application in radiotherapy, especially in treatment planning. Thinking about maximizing information in an image, image registration has been found to be handy, though computationally expensive to achieve. In this work, we describe an experiment to help establish a relationship between registration performance and the extent of misalignment that made registration necessary using data from a CT scan of the body. We present ways in which information measures can be used to decide whether registering images is a necessary operation. We visualize the experimental result and define functions that fits the distribution by making an educated guess and then optimized the functions to arrive at as minimum parameter as possible. We finally screen the various models to arrive at the optimally performing ones. We have found these models to perform very well in predicting registration performance pre-operationally, explaining between ~62.94% to ~99.96% of the effect of rotating around or translating along x, y, z on the performance of registration output should it be carried out, thereby saving more computer power required in image registration, time and boredom on the part of the patient.

**Corresponding author: E-mail: adelekeabayo@gmail.com;*

Keywords: Image; image information; image registration; entropy; prediction.

1. INTRODUCTION

Imaging techniques over the years have become indispensable tools in medicine and clinical sciences. They are fast becoming an important diagnostic tool for in-vitro examination of living tissues and organs in an organism. For example, it was submitted that x-ray images are images of a measure of the distribution of attenuation coefficients at a given average x-ray energy within a tissue. As imaging techniques advances, so also is the need to compare results and information from them [1,2,3]. Furthermore, Image information content was discussed as an intrinsic property of an image. Image information is not subject to human impression, but is solely determined by the available image data [4]. Thus image information content can be defined as a set of recursive descriptions of discernable image data structures perceived at different visibility levels. Other authors define image information as a measure of average uncertainty (randomness) in an image. To measure the information in an image, according to these authors, the entropy of the image histogram is measured [4,5].

Image registration, otherwise called image alignment is no new task in image processing. It is a fundamental procedure used to match two or more pictures taken either at different times (multi-temporal), from different spatial directions (multi-view) or by using different imaging techniques (multi-modal). The goal of image registration is to find the optimal transformation that best aligns the structures of interest in the input images [6]. The idea behind the task of integrating two or more images gotten from different procedures or time is the fact that each of the images carries unique information which can be complementary [7].

Over the last twenty years, mathematicians and image processing scientists around the world have developed novel algorithms for registering images. These algorithms have been independently studied for several different applications which have given birth to a rather compelling research outputs. The fact still remains that none of these existing procedures is self-contained. While solving a particular problem, they often than not create other problems like amplification of noise in the output. Thus, the question is no longer how do we register images, but rather how efficiently and fast are we achieving registration. In this work, a 'registered image' refer to the image obtained by matching two images taken either at different time, viewpoints or modalities and 'unregistered image' refer to the image that have not been registered with any other image.

As part of the routine at iThemba LABS, a patient's x-ray is taken and digitally reconstructed radiographs (DRRs) are generated using data built-up during routine CT scan of the patient in preparation for radiotherapy. The x-ray and DRR are compared through a process of image registration which searches for an optimal transformation to align the CT coordinate system with that of the operating room. This process takes a long time before it is completed. By extension, the longtime of image registration translates directly into a longer treatment time. This makes the process of radiotherapy tiring for patients. Since image registration can be an expensive operation, identifying problematic views is very important. The work here uses the novel tool of computational experiment to come up with models that can predict the performance of Image registration pre-operationally. Volume of models are presented, which were screened using their statistical performances. From thorough review of literature, Information measures upon which predictions can be based were found and a discussion on how to make sense of these results are also presented. Thus with these models, it can be decided whether a patient require registration during treatment or not, thereby saving time and Computer power.

2. REVIEW OF RELATED LITERATURE

An image is a two dimensional function f(x,y), where x and y are spatial coordinates and f is an amplitude signifying the gray level (intensity) at a given pair of coordinates x,y [8]. Gray level digital image is the class of images to which digitally reconstructed radiographs (DRR) and x-ray radiographs belong and can be processed in three ways. These operations are identified as point operation, arithmetic operation and geometric image operation. Point operations are applied to individual pixels only. This type of operation does not take into consideration the correlations between two neighbouring pixels. The basic tool used for defining point operations on a digital image is the image histogram, given explicitly by

$$H_f(k) = J \tag{1}$$

Where H_f is a one-dimensional function with domain {1,⋯ ,K} and possible range extending from 1 to the number of intensities plus one (K +1) in the image. J is the occurrences of gray level k for each k = 1,⋯ ,K. Noise reduction and the detection of how the movement rate of an image changes can be accomplished through arithmetic operation between images of the same spatial dimension. However, geometric image operation complement point operation because they are refined as a function of spatial position only as-opposed to both image intensity and spatial location [9].

In further works, authors have redefined image registration as a process of aligning images (radiographs) into a common coordinate system, so that a simple change between the images can be identified [7]. It is described as the task of setting up correspondence between two or more images. Thus, image registration spans the whole process of putting images together for the purpose of getting a single image which explains the object more completely than any of the individual images [1,10]. One of the sources of dissimilarity in medical images was identified as occlusion, which occur when some part of the tissue being imaged are masked either by some growth or diffusion of contrast agent. Other sources of dissimilarity include: Poor acquisition conditions, obstruction, error in patient alignment with source of radiation during imaging and contrast change. Image registration could be an interesting tool in planning treatments. One of such application is when the image of a patient's organ is taken using more than one modality. For example, magnetic resonance imaging (MRI) can be used to give an excellent anatomical structure of the organ, while single photon emission computed tomography (SPECT) can be used to give an excellent functional structure [2,3]. However, if the two images can be aligned, the functional information of SPECT can be localized using MRI image which gives a result that contain improved diagnostic information and can be used for better treatment planning [10]. Image registration can be classified into the following groups:

1. Correlation and Sequential Method: This method is particularly useful for images which are misaligned by small rigid of affine transformations. A transformation is affine if T(x)−T(0) is linear. This method has been found to be immensely useful in the registration of mono-modal images [7]. If given a reference and referred images with entropy R and I respectively, where R < I, then the normalized 2-dimensional cross correlation function, which measures the similarity of each transformation is given as [5,11]:

$$C(u,v) = \frac{\sum_x \sum_y R(x,y) I(x-u, y-v)}{\sqrt{\left[\sum_x \sum_y R^2 (x-u, y-v)\right]}} \quad (2)$$

The cross correlation is normalized to avoid its value being altered by local image intensity. The function C(u,v) is maximized for the transformation at which the reference image matches the referred image exactly. In a further works, attention was drawn to the fact that entropy correlation coefficient (ECC) can be used to obtain a keen image registration using normalized mutual information. However, it is worthy of note that as much as cross correlation is a primary tool for correlation and sequential method of registration, it is by itself not a registration method. It is a fundamental statistical approach to registration. It performs best when used as a similarity measure or match metric [11,12].

2. Fourier-Mellin Method: This is a scene, sensor and illumination independent method of registration. This method searches for optimal match according to the information of the image in the frequency domain. This makes the method efficient and resistant to correlated and frequency-dependent noise. However, the Fourier-Mellin method of registration is applicable to images that are misaligned due to translation and rotation. The Fourier transform is applied to images to recover translation while phase correlation is applied to recover rotation angle of a misaligned image, using phase correlation in the log polar space [13,14]. From Fourier analysis, we already know that the Fourier transform of an image f(x,y) is a complex function with a real and imaginary component, $R(\omega_x, \omega_y)$ and $I(\omega_x, \omega_y)$ respectively at each spatial frequency (ω_x,ω_y) of the frequency spectrum:

$$F(\omega_x, \omega_y) = R(\omega_x, \omega_y) + jI(\omega_x, \omega_y) \quad (3)$$

equivalently,

$$F(\omega_x, \omega_y) = |F(\omega_x, \omega_y)| e^{j\phi(\omega_x, \omega_y)} \quad (4)$$

with $|F(\omega_x, \omega_y)|$being the amplitude of the Fourier transform and $\phi(\omega_x, \omega_y)$, the phase angle

[13,14]. The phase angle describes how much of the phase shifts at each frequency. It is define as:

$$\phi(\omega_x, \omega_y) = tan^{-1}\left(\frac{I(\omega_x, \omega_y)}{R(\omega_x, \omega_y)}\right) \quad (5)$$

Details of the implementation of this method of registration is contain in the work of [13,14]. The peculiar property of the Fourier analysis that is being explored in the Fourier-Mellin method of registration is the well-known Fourier shift property.

3. Point Mapping Method: This is also known as the landmark mapping technique. The method is specifically useful for registering two images whose type of misalignment is unknown. In other words, in these images, the class of transformation cannot be conveniently categorized as a set of small translation or rigid-body movements. Thus, the technique tends to harness the landmarks present in the two images, matched through a more general transformation. The process consists of basically three processing stages. First, features in the images are computed. This is followed by the matching of features from reference image, also known as the control point, to the referred image. Finally, the spatial mapping of the control points to the features in the referred image through the use of 2-d polynomial function of specified order. Hence, through interpolation of the mapped features, re-sampling of referred image into reference image is achieved [14].

4. Mutual Information-based Method: This method symbolises the foremost technique in multimodal registration. It makes use of information theoretic measures such as mutual information. This method is most applicable in solving correspondence problem in feature-based registration. It estimates the joint probability of intensities of voxels corresponding to one another in two images [15]. The amount of information that one random variable in one image contain about another in the second is referred to as the mutual information between the two images. If we consider the information content of one image as a set H(X) and the information content of another image as a set H(Y), the mutual information is the intersection of set H(X) and H(Y) as shown in the Fig. 1.

In practice, one can transform any image I and image J into a random variable. If we write p(i) for the probability density function of random variable I in image I, p(j) for the probability density function of random variable J in image J and p(i,j) for the joint probability density of I and J, then the mutual information of the two images I and J is given as [15]:

$$M(I,J) = \sum_{i\epsilon I}\sum_{j\epsilon J} P(i,j) log_2 \frac{p(i,j)}{p(i)p(j)} \quad (6)$$

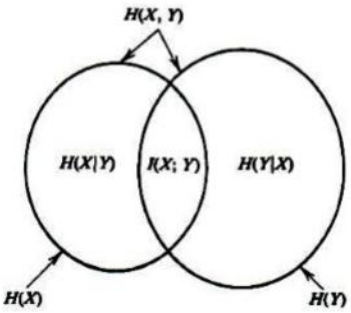

Fig. 1. Relationship between entropy and mutual information [15]

3. EXISTING MODELS AND METHODS OF IMAGE INFORMATION MEASURE AND THEIR APPLICATION TO PRESENT WORK

1. Gabor Filtering: This image performance method can be used to assess and compare the effectiveness of different methods of acquisition or processing of the images. It was argued that the well-known Peak Signal to Noise Ratio (PSNR) and Mean Square Error (MSE) method of assessing the performance of image processing has recorded little success and failed in a rather enormous way because it lacks the frame work to measure the human observer perceived quality. Thus, towards obtaining a robust model with better performance, method based on the use of the Human Visual System (HVS) was suggested [16]. Daugman in his work uncovered filtering of images using Gabor filters. These filters were modelled to behave like a simple cortical cell in the visual system when responding to input signal (preferably an image). The Gabor filter according to him is given as [16]

$$G_{\theta,f,\sigma_1,\sigma_2}(x,y) = exp\left[-\frac{1}{2}\left(\frac{x'^2}{\sigma_1^2}+\frac{y'^2}{\sigma_2^2}\right)\right]\cos(2\pi f x' + \phi) \quad (7)$$

where $x' = x\sin\theta + y\cos\theta$ and $y' = x\cos\theta + y\sin\theta$, σ_1 is the standard deviation of pixel distribution in the first image acquired through a particular mode and σ_2 is the standard deviation of pixel distribution in the second image acquired through another mode. ϕ is the phase difference between the two images being analyzed. Equation (7) can be thought of as an amplitude modulated plane wave with an amplitude of the form of a 2−d Gaussian envelop. Furthermore, f is the spatial frequency of the wave at an angle θ to the x−axis. The algorithm involves passing the image through banks of Gabor filters to extract textural and contour information from it, thereby converting it to Human Visual System (HVS) domain [17]. This is followed by quantification of information content measure of the filtered image, achieved by evaluating the information entropy of the image characterized by its histogram as below [16,17].

$$H(I) = -\sum_{x=1}^{m}\sum_{y=1}^{n} hist_{norm}(L)\log\left(hist_{norm}(L)\right) \quad (8)$$

where L represents the intensity levels of the m×n image I(x,y) and $hist_{norm}(L)$ is the normalized histogram constrained to $\sum_x hist_{norm}(L) = 1$. As a follow up, Vazquez-Fernandez and his group choose the following parameters: $\theta \in \left[0, \frac{\pi}{6}, \frac{\pi}{3}, \frac{\pi}{2}, \frac{2\pi}{3}, \frac{5\pi}{6}\right]$which was later discovered to have played an insignificant role in the image processing. The entropy evaluation was followed by normalization of the Gabor responses according to the type of filter with respect to phase [16]. Two phases $\phi_1 = 0$ and $\phi_2 = \frac{\pi}{2}$ were used for symmetric and anti-symmetric filters respectively. The energy of the filtered images was given by [16].

$$E(x,y) = \sqrt{R_{\phi_1}(x,y)^2 + R_{\phi_2}(x,y)^2} \quad (9)$$

Where $R_{\phi_i}(x,y)$ is the Gabor response for the phase ϕ_i. Based on the fact that the entropy calculated from the Gabor filtered image is not absolute, the model proposed the evaluation of a relative quality metric Qr. This is computed by taking the average of the entropy of energies of all the Gabor filtered images under consideration. The reference images are also processed without the use of the Gabor filter. The average of the entropy of the images are taken as well. The average entropy of the reference image is then multiplied by the inverse of the average energy entropy of the Gabor filtered image as

$$H_{ref} = \frac{1}{N}\sum_{i=1}^{N} H_{ref_i}$$

$$H = \frac{1}{N}\sum_{i=1}^{N} H_i$$

$$Q_r = \frac{H_{ref}}{H} \quad (10)$$

The standard deviation of the Gaussian envelop of the plane wave was fixed to $\frac{\tau}{2}$. Finally, two spatial frequencies, f1 and f2, were chosen as a function of the spatial period τ i.e f1 for τ ∈{8} and f2 for τ ∈{4} [16,17].

Application of the model to the present work: We used this model to predict image registration performance by having two sets of radiographs; Registered and Unregistered. The unregistered radiograph was marked as the reference and the registered as referred image. The average entropy of each of these two images was evaluated and the quantity Qr as given in Equation (10) was evaluated. Then the following interpretations apply.

(a) Qr< 1: The registration is worthwhile because the entropy of the registered image will be higher than that of the reference image. The numerical value quantitatively describes the performance of the registration algorithm.
(b) Qr≥ 1: The registration is not worthwhile because the entropy of the registered image will be lower than that of the reference (unregistered) image. The numerical value quantitatively describes the performance of the registration algorithm.

2. Transmitted Information (TI): The major concern of medical image processing, which has formed a cardinal focus of research in the field of image processing is the way measurement of some parameters such as noise content affects image quality. Tsai presented and discussed how information theoretic quantities can be used to describe how much information is contained in a given image. They presented a methodology that uses transmitted information which combines

assessment of noise and resolution by a single number, rather than mutual information that has dominated research in the field of medical image processing since the early 1990s [18]. For further reading, details of this experiment can be found in literature [18]. TI is the amount of information transmitted from the input image to the output image. Equation (11) was presented for evaluating this parameter from radiographic images.

$$T(x,y) = H(x) + H(y) - H(x,y) \quad (11)$$

Where H(x) is the information entropy of the input image, H(y) is the information entropy of the output image and H(x,y) is the joint entropy of both input and output images [18].

Application of the model to the present work: This model was used to predict the performance of an image registration procedure and we decided based on the outcome from the model whether registration was necessary in the first place. Let us have two sets of radiographs; registered and unregistered (reference). The unregistered radiograph is marked as input and the registered radiograph as output. The average entropy of each of these two images was evaluated, and marked as H(i) and H(o) respectively. The quantity H(i,o) which is the joint entropy of both the input and the output images is evaluated as well. Finally, the transmitted information T(i;o) was evaluated according to Equation (11). Then the following interpretations apply.

(a) T(i;o) ≤ H(i): The registration is not worth while because the information that is transmitted from the unregistered image to the registered image during registration is quite less or the same as the actual information content of the unregistered image. Thus, the registered image is not an enhanced form (in term of information content) of the unregistered image. The quantitative performance of the registration procedure is thus the value of T(i,o).

(b) T(i;o) > H(i): The registration is worthwhile because the information that is transmitted from the unregistered image to the registered image during image registration is more than the actual information content of the unregistered image.

3.1 iTHEMBA LABS

iThemba Laboratory for Accelerator Based Sciences (LABS) is the primary centre of expertise in radiation medicine and nuclear science and technologies to advance the knowledge and health of the people of Africa and is the only particle therapy facility in Africa. In an attempt to develop a patient positioning system for high precision radiation therapy, much research has been done in the area of image processing within the institute. Efforts from cutting edge research has given birth to the iThemba LABS Digitally Reconstructed Radiograph (DRR) generation system and the iThemba LABS image registration system. Images used for the implementation and model testing in this work are all generated using the iThemba LABS Digitally Reconstructed Radiograph (DRR) generation system. In radiotherapy, and ultimately in patient treatment planning, problematic views such as misalignment, noise or poor lightening are not acceptable. Therefore, image registration minimizes this problem.

3.1.1 The system at iTHEMBA labs

3.1.1.1 DRR generator

The DRR generation program is a C + + program. The Graphical User Interface(GUI) takes the following as input:

(a) CT Cube: This enables the user to load the patient's header file into the program. This file contain the image information of a specific site of a patient. The header file is written during routine CT scan of a patient. The Load CT Cube button is used to implement the header file into a form that is suitable for radiograph generation.

(b) DRR Parameters: This takes as input, three (3) translational parameters and three (3) rotational parameters. These are translational parameters along the x, y and z axes alongside with rotational parameters along the x, y and z axes. This can be represented as (x,y,z,θx,θy,θz).

(c) Contrast: The contrast level of the image to be generated can be specified on a scale of 0 to 150. After the prompts above have been specified, the Generate DRR command button is hit to execute the generation program. The output from this program is a DRR that satisfy all the specified parameters.

3.1.1.2 Image registration system

The Image Registration System is a C++ program. The Graphical User interface takes the following as input:

(a) Reference Image: This enable user to load a reference image that is assumed to be correctly aligned and with acceptable contrast. The reference image can be a DRR generated with correct parameters or a digital x-ray file.
(b) CT Cube: This enables the user to load the patient's header file into the program. The Load CT Cube button is used to implement the header file into a form that is suitable for radiograph generation.
(c) Parameters to start registration with: This takes as input, three (3) translational parameters and three (3) rotational parameters. These are translational parameters along the x, y and z axes alongside with rotational parameters along the x, y and z axes. That is (x,y,z,θx,θy,θz). The parameters are chosen so that they correspond to the one used for the generation of referred image. After the prompts above have been specified, the Register command button is hit to execute the registration program. The output from this program is a DRR that satisfy an optimized registration.

3.2 Class of Problems

As it was considered in this work, image registration problem source is divided into two main parts:

3.2.1 Alignment problem

This arises when there is an offset in the referred image along one or more of the translational axes (x,y,z) from the reference image. An offset along one or more of the rotational axes (θx,θy,θz) can also be a source of alignment problem which makes image registration an important operation.

3.2.2 Contrast problem

This arises when there is an offset in the contrast of the referred image, making it different from the reference image. This problem may cause a blurry or unclear image of a tumour for which a patient is being prepared for treatment as observed in Fig. 2.

The experimental set up in this work was such that help to generate data which was used to model image information measure. Data was generated from registered images using the registration system described above as a function of each of these registration problem sources.

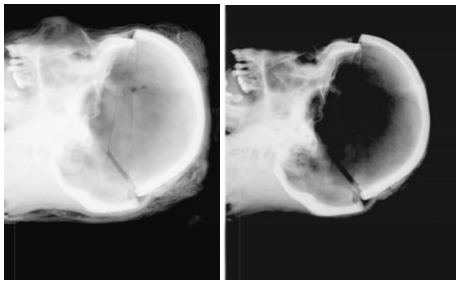

(a) (b)

Fig. 2(a). Low information radiograph, H(I) = 5.85 bits, (b) High information radiograph, H(I) = 6.32 bits [19]

4. METHODOLOGY

Models in this work were developed based on data from CT scan of the body and assessing the results on anterior/posterior x-ray views. It involved visualizing the experimental result followed by defining functions that fits the distribution by making an educated guess and then optimizing the functions to arrive at as minimum parameter as possible. It also involved testing some of the models that were developed. This helps to know how well the models predict image registration performance. A number of tests were conducted to evaluate the performance of the image registration algorithm implemented and operational at iThemba LABS. The distributions of these performances were then used to design a robust model useful for prediction. Carstens, a postgraduate student showed that his proposed DRR generation and image registration systems are efficient [20]. His argument and novelty of his work led to the implementation of the system at iThemba LABS. The experiment in this work was designed to predict the performance of Carsten's system, with the aim of evaluating it effectiveness and ultimately decide whether or not the output from this system is worth the computation cost for a given set of good and corrupted type of the same image. This will help to decide whether or not registration is necessary during treatment.

5. EXPERIMENT

The prediction of the performance of the image registration system being considered in this work was achieved relative to the DRR generation system operational at iThemba LABS, using the Mutual Information (MI), Garbor Filtering's entropy quotient (Qr) and Transmitted Information (TI) techniques described by equation (6), equation (10) and equation (11) respectively.

5.1 Similarity Tests

For the first cycle of experiments, the similarity measurements were taken for movement along the six dimensions (3-translation and 3-rotation) in the parameter space, for a fixed contrast. The different dimensions are all limited to between 0−5mm or between 0−50 degrees. The second cycle of experiments was designed so that the similarity measurements are taken for movement along six dimensions in the parameter space of the registered image, while varying the contrast of the reference image. The different contrasts are limited to integer values between 50 and 150. In this work, six sets of experiments were done, with each configuration showing the effect of simultaneous variation of contrast and misalignment in one dimension. Contrast change was done between 50 and 150 at a step length of 10. For each run of the experiment, the reference image was maintained at a contrast level of 50 and with {40.0,36.0,120.0,0.0,0.0,0.0} parameters in the parameter space while changing the parameter values of each of the parameters in the parameter space (one at a time) for the referred images. The parameters in the parameter space were changed between 0 and 4.5 at a step length of 0.5 degrees and millimetres for the rotation and translation parameters respectively. The experiment was designed and implemented using a single data file, representing one patient. The idea is to validate the model built from one patient with other patients to ensure that we have a working model that successfully captured the effect of simultaneous contrast change and misalignment on image registration performance. Fig. 3 shows a sample DRRs used for the experiment.

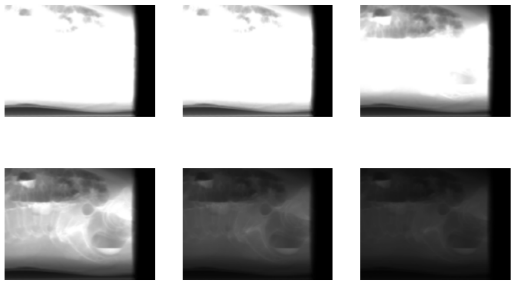

Fig. 3. The first image in the set of images above is the reference image, while the second image to the 6th image are the referred images. Each of the referred images is 40 contrast level higher than the previous, with the first referred image having the same contrast as the reference image - 50, hence no contrast offset [21]

5.2 Experimental Assumptions

This experiment was designed based on the assumption that the information measures being investigated are a function of only one independent but deterministic variable from the parameter space and the contrast. This assumption simplifies the data sets from the experiment suitable for modeling with simple functions. Examples of such models are monomial or linear combination of monomials (polynomial) of a single independent variable and linear combination of wave functions with harmonics. The experiment assumes that during treatment planning, the referred image is misaligned on one parameter in a parameter set. Since we expect the transmitted information (TI) and mutual information (MI) of the reference image and the registered image to be the same as the entropy of the reference image, we expect the variation of the information measures to be strictly dependent on the misaligned parameter. If there is no misalignment between the reference and referred image, the entropy quotient Qr is expected to be unity.

5.3 Linear Models

In the science of forecasting, prediction and modeling, the need to mathematically characterize the behaviour of a system (ranging from simple one like force acting on a spring to complex one as a population dynamic in an ecological system) cannot be ruled out. The method of the least squares helps us to find the best fit line to a given data sets. Results from the experiment designed above were used to develop linear models which can represent the relationship that exists between the dependent variables and independent variables such as rotation, translation and contrast. The tool employed in this work for parameter estimation and model verification is the least squares method of estimation [22].

5.4 R-squared Value

Being a statistical measure is an indication and measure of the closeness of fitted regression line to data points. It is popularly referred to as coefficient of determination. It is the percent of variance explained by the model, that is the square of the correlation between the dependent and the independent variable [23]. In this work, the R-squared value is the square of the

correlation between the information measure and the source of misalignment explaining it.

$R^2 = 1 -$ (*sum of squared distance between Reference image variables and refered image variables / sum of squared distance between Reference image variables and their mean)*

(11a)

It will be interpreted as a percentage rather than a decimal number.

5.5 The Standard Error

The standard error of a certain sample statistic is formally defined as the standard deviation of that statistic, assuming that a large number of samples is gathered [24]. The standard error estimators associated with widely used descriptive statistic and in this work is given as:

$$S_E = \frac{S_D}{\sqrt{2(n-1)}} \tag{11b}$$

$$S_D = \sqrt{\frac{1}{n-1}\sum_{i=1}^{n}(X_i - \bar{X})^2} \tag{11c}$$

Where S_E is the standard error, S_D is the standard deviation, X_i is the ith observation in the distribution, $\bar{X}$ is the mean of the distribution and n is the number of observation for $n \leq 40$ as is the case in this work.

5.6 Likelihood Estimation

If we define a function which mathematically describes the process underlying the observed samples of data (MI, TI and Qr), and the generating process as f(y|θ) where θ = {a,b,⋯} as the case maybe, then the joint density of n independent and identically distributed observations from this process is the product of individual densities;

$$f(y_1, \ldots y_n|\theta) = L(\theta|y) = \prod_{i=1}^{n} f(y_i|\theta) \tag{11d}$$

The log-likelihood function given by:

$$\ln L(\theta|y) = \sum_{i=1}^{n} \ln f(y_i|\theta) \tag{11e}$$

is however simpler to work with. For the purpose of emphasis, it suffices to write

$$L(\theta|y) = L(\theta|data) \tag{11f}$$

The likelihood and the log-likelihood evaluated at θ is given by equation (11d) and equation (11e) respectively [25].

6. MODEL COMPARISON AND SELECTION

Choosing a best performing model amongst well competing models to describe a data set is challenging. There are different types of information criterion, with each suitable for models developed under some specific assumptions. These criteria include the Takeuchi's Information Criterion (TIC) developed in 1976 for comparing models particularly not close to truth, Bayelsian Information Criterion (BIC), the Akaike's Information Criterion (AIC) and the Akaike's Second-order Corrected Information Criterion (AICc). During the last fifteen years, Akaike's entropy-based Information Criterion (AIC) has had a fundamental impact in statistical model evaluation problems. The extensions of AIC to AICc make AIC asymptotically consistent and penalize over parameterization more stringently to pick only the simplest of the "true" models. The criterion is defined as [26,25]:

$$AIC = -L_q + q \tag{11g}$$

where Lq is the maximized log-likelihood for an estimated model with q number of parameter. He further buttressed that when a model is fitted to experimental data (as employed in this work), the criterion is redefined as [26,25]:

$$AIC = -2L_q + 2q \tag{11h}$$

In a case where the number of observation is very small relative to the number of parameters (say n q < 40), the modified Akaike's Information Criterion as given in equation (11h) become inappropriate due to the bias associated with the small size of n. However, the bias is compensated in the corrected version of the originally modified AIC. The Akaike's second-order corrected information criterion extends the AIC as [26,25]:

$$AICc = AIC + 2q(q+1)(n-q-1) \tag{11i}$$

For this work, we used AICc to compare our proposed models for predicting the performance of an image registration procedure. To select the best performing one, we used the R-squared

value. This choice is not only because we have used the method of least squares to fit our proposed models to data, but because we worked also with an assumption that our data is independent and identically distributed (that is, a given similarity measure in the set of possible measures in an image is independent of the random but determinable variables, such as sources of misalignment, preceding it) due to the system. Our choice of AICc is hinged on the fact that, added to its ability to perform best in a case where the number of observation is very small relative to the number of parameters, say $\frac{n}{q} < 40$ where n is the number of observations and q is the number of parameters, it is also an information criterion suitable for comparing models with different error distribution which is the case in our models. Furthermore, AICc is also a suitable information criterion for nested models, which is the case of the two harmonic models used in this work.

6.1 Similarity Measures for Rotation with Varying Contrast

The models below were proposed for predicting the mutual information and by extension, the transmitted information between the reference image and the registered image:

$$MI(I,J,\alpha,\theta_x,\phi) = H(I,\alpha) + \beta\sin\left(\frac{2\pi\theta_x}{\phi}\right) + \gamma\cos\left(\frac{2\pi\theta_x}{\phi}\right) \quad (12)$$

$$MI(I,J,\alpha,\theta_x,\phi) = H(I,\alpha) + \beta\sin\left(\frac{2\pi\theta_x}{\phi}\right) + \gamma\cos\left(\frac{2\pi\theta_x}{\phi}\right) + SH \quad (13)$$

$$MI(I,J,\alpha,\theta_x) = a\theta_x^4 + b\theta_x^3 + c\theta_x^2 + d\theta_x + H(I,\alpha) \quad (14)$$

Where $MI(I,J,\alpha,\theta_x,\phi)$ is the mutual information shared between reference image I and registered image J, $H(I,\alpha)$ is the information entropy of I with contrast α. θ_x is the degree of rotation of the misaligned image from the reference image around the x axis, ϕ is the period of oscillation of the mutual information with changing θ_x . Furthermore, β, γ, a, b, c, d are coefficients that are system dependent and SH is the second harmonic terms. In the case of misalignment around the y and z axes, θ_x is replaced with θ_y and θ_z respectively in the new model.

The models below were proposed for predicting the entropy ratio Qr between the registered J image and misaligned image R.

$$Q_r(J,R,\alpha,\theta_x,\phi) = K(J,R,\alpha) + \gamma\cos\left(\frac{2\pi\theta_x}{\phi}\right) \quad (15)$$

$$Q_r(J,R,\alpha,\theta_x,\phi) = K(J,R,\alpha) + \beta\sin\left(\frac{2\pi\theta_x}{\phi}\right) + \gamma\cos\left(\frac{2\pi\theta_x}{\phi}\right) + \rho\cos\left(\frac{4\pi\theta_x}{\phi}\right) \quad (16)$$

$$Q_r(J,R,\alpha,\theta_x) = a\theta_x^3 + b\theta_x^2 + c\theta_x + K(J,R,\alpha) \quad (17)$$

Where

$$K(J,R,\alpha) = 1 - \frac{H(R,\alpha)}{H(J,\alpha)} \quad (18)$$

And ρ is a coefficient that is system dependent.

When there is a misalignment due to rotation around the y axis only, we propose the following models for predicting the mutual information between the reference image and the registered image:

$$MI(I,J,\alpha,\theta_y,\phi) = H(I,\alpha) + \beta\sin\left(\frac{2\pi\theta_y}{\phi}\right) + \gamma\cos\left(\frac{2\pi\theta_y}{\phi}\right) \quad (19)$$

$$MI(I,J,\alpha,\theta_y,\phi) = H(I,\alpha) + \gamma\cos\left(\frac{2\pi\theta_y}{\phi}\right) + \rho\sin\left(\frac{4\pi\theta_y}{\phi}\right) \quad (20)$$

$$MI(I,J,\alpha,\theta_y) = a\theta_y^4 + b\theta_y^3 + c\theta_y^2 + d\theta_y + H(I,\alpha) \quad (21)$$

And the following models for predicting the entropy ratio of registered image and misaligned image.

$$Q_r(J,R,\alpha,\theta_y,\phi) = K(J,R,\alpha) + \beta\sin\left(\frac{2\pi\theta_y}{\phi}\right) + \gamma\cos\left(\frac{2\pi\theta_y}{\phi}\right) \quad (22)$$

$$Q_r(J,R,\alpha,\theta_y,\phi) = K(J,R,\alpha) + \beta\sin\left(\frac{2\pi\theta_y}{\phi}\right) + \gamma\cos\left(\frac{2\pi\theta_y}{\phi}\right) + \rho\cos\left(\frac{4\pi\theta_y}{\phi}\right) \quad (23)$$

$$Q_r(J,R,\alpha,\theta_y) = a\theta_y^2 + b\theta_y + c + K(J,R,\alpha) \quad (24)$$

ρ is a coefficient that is system dependent.

However, if the misalignment is due only to rotation around the z axis, we propose the following models for predicting the mutual information between the reference image and the registered image:

$$MI(I,J,\alpha,\theta_z,\phi) = H(I,\alpha) + \beta\sin\left(\frac{2\pi\theta_z}{\phi}\right) + \gamma\cos\left(\frac{2\pi\theta_z}{\phi}\right) \quad (25)$$

$$MI(I,J,\alpha,\theta_z,\phi) = H(I,\alpha) + \beta\sin\left(\frac{2\pi\theta_z}{\phi}\right) + \gamma\cos\left(\frac{2\pi\theta_z}{\phi}\right) + SH \quad (26)$$

$$MI(I,J,\alpha,\theta_z) = a\theta_z^5 + b\theta_z^4 + c\theta_z^3 + d\theta_z^2 + e\theta_z + H(I,\alpha) \quad (27)$$

Where e is a coefficient that is system dependent. Similarly, the following models for predicting the entropy ratio of registered image and misaligned image.

$$Q_r(J,R,\alpha,\theta_z,\phi) = K(J,R,\alpha) + \beta\sin\left(\frac{2\pi\theta_z}{\phi}\right) + \gamma\cos\left(\frac{2\pi\theta_z}{\phi}\right) \quad (28)$$

$$Q_r(J,R,\alpha,\theta_z,\phi) = K(J,R,\alpha) + \gamma\cos\left(\frac{2\pi\theta_z}{\phi}\right) + \rho\sin\left(\frac{4\pi\theta_z}{\phi}\right) \quad (29)$$

$$Q_r(J,R,\alpha,\theta_z) = a\theta_z^3 + b\theta_z^2 + c\theta_z + K(J,R,\alpha) \quad (30)$$

6.2 Similarity Measures for Translation with Varying Contrast

The models below are proposed for predicting the mutual information and by extension, the transmitted information between the reference image and the registered image (the image gotten by registering an image misaligned by a translation along the x axis only, with the reference image):

$$MI(I,J,\alpha,x,\phi) = H(I,\alpha) + \beta\sin\left(\frac{2\pi x}{\phi}\right) + \gamma\cos\left(\frac{2\pi x}{\phi}\right) \quad (31)$$

$$MI(I,J,\alpha,x,\phi) = H(I,\alpha) + \beta\sin\left(\frac{2\pi x}{\phi}\right) + \gamma\cos\left(\frac{2\pi x}{\phi}\right) + SH \quad (32)$$

$$MI(I,J,\alpha,x) = ax^4 + bx^3 + cx^2 + dx + H(I,\alpha) \quad (33)$$

Where $MI(I,J,\alpha,x,\phi)$ is the mutual information shared between reference image I and registered image J, H(I,α) is the information entropy of I with contrast α. x is the length of translation of the misaligned image from the reference image along the x axis, $\phi$is the period of oscillation of the mutual information with changing x. Furthermore, β , γ , a, b, c, d are coefficients that are system dependent and SH is the second harmonic terms. In case of misalignment along the y and z axes, x is replaced with y and z respectively in the new model. To predict Q_r between the registered image and misaligned image, we propose the following models:

$$Q_r(J,R,\alpha,x,\phi) = K(J,R,\alpha) + \beta\sin\left(\frac{2\pi x}{\phi}\right) + \gamma\cos\left(\frac{2\pi x}{\phi}\right) \quad (34)$$

$$Q_r(J,R,\alpha,x,\phi) = K(J,R,\alpha) + \varrho\sin\left(\frac{4\pi x}{\phi}\right) + \rho\cos\left(\frac{4\pi x}{\phi}\right) \quad (35)$$

$$Q_r(J,R,\alpha,x) = ax^3 + bx^2 + cx + K(J,R,\alpha) \quad (36)$$

When there is a misalignment due to translation along the y axis only, we propose the following models for predicting the mutual information between the reference image and the registered image:

$$MI(I,J,\alpha,y,\phi) = H(I,\alpha) + \beta\sin\left(\frac{2\pi y}{\phi}\right) + \gamma\cos\left(\frac{2\pi y}{\phi}\right) \quad (37)$$

$$MI(I,J,\alpha,y,\phi) = H(I,\alpha) + \beta\sin\left(\frac{2\pi y}{\phi}\right) + \gamma\cos\left(\frac{2\pi y}{\phi}\right) + SH \quad (38)$$

$$MI(I,J,\alpha,y) = ay^3 + by^2 + cy + H(I,\alpha) \quad (39)$$

We propose Q_r to be predicted using:

$$Q_r(J,R,\alpha,y,\phi) = K(J,R,\alpha) + \beta\sin\left(\frac{2\pi y}{\phi}\right) + \gamma\cos\left(\frac{2\pi y}{\phi}\right) \quad (40)$$

$$Q_r(J,R,\alpha,y,\phi) = K(J,R,\alpha) + \rho\sin\left(\frac{2\pi y}{\phi}\right) + \gamma\cos\left(\frac{2\pi y}{\phi}\right) \quad (41)$$

$$Q_r(J,R,\alpha,y) = ay^3 + by^2 + K(J,R,\alpha) \quad (42)$$

When there is a misalignment due to translation along the z axis only, we propose the following models for predicting the mutual information between the reference image and the registered image:

$$MI(I,J,\alpha,z,\phi) = H(I,\alpha) + \beta\sin\left(\frac{2\pi z}{\phi}\right) + \gamma\cos\left(\frac{2\pi z}{\phi}\right) \quad (43)$$

$$MI(I,J,\alpha,z,\phi) = H(I,\alpha) + \beta\sin\left(\frac{2\pi z}{\phi}\right) + \gamma\cos\left(\frac{2\pi z}{\phi}\right) + SH \quad (44)$$

$$MI(I,J,\alpha,z) = az^5 + bz^4 + cz^3 + dz^2 + ez + f + H(I,\alpha) \quad (45)$$

Where f is a coefficient that is system dependent. We propose $Q_r$to be predicted using:

$$Q_r(J,R,\alpha,z,\phi) = K(J,R,\alpha) + \beta\sin\left(\frac{2\pi z}{\phi}\right) + \gamma\cos\left(\frac{2\pi z}{\phi}\right) \quad (46)$$

$$Q_r(J,R,\alpha,z,\phi) = K(J,R,\alpha) + \beta\sin\left(\frac{2\pi z}{\phi}\right) + \gamma\cos\left(\frac{2\pi z}{\phi}\right) \quad (47)$$

$$Q_r(J,R,\alpha,z) = az^2 + bz + K(J,R,\alpha) \quad (48)$$

7. RESULTS

The observations made during experimentation are described using optimised and generalized linear models. These models describe the relationship between the quantity being measured and the parameter. The result is therefore presented in subsections based on the three classes of varying parameters: rotation, translation and contrast.

7.1 Similarity Measures for Rotation with Varying Contrast

The model statistics for equation 12 - 17 is as shown in Table 1.

The model statistics for equation 19 – 24 is as shown in Table 2.

The model statistics for equation 25 - 30 is as shown in Table 3.

7.2 Similarity Measures for Translation with Varying Contrast

The model statistics for equation 31 - 36 is as shown in Table 4.

The model statistics for equation 37 – 42 is as shown in Table 5.

The model statistics for equation 43 - 48 is as shown in Table 6.

Table 1. Model statistics for θ_x

Info. measure	Model	Statistics				
		Standard error	R-squared	P-value	AICc	Degree of freedom
	Eqn 12	0.01322	0.3238	0.2542	-45.7	7
MI	Eqn 13	0.01015	0.7151	0.1207	-30.4	5
	Eqn 14	0.009948	0.7265	0.1102	-30.8	5
	Eqn 15	0.0001379	0.8889	4.371e-05	-141.6	8
Q_r	Eqn 16	5.765e-5	0.9854	6.722e-06	-147.0	6
	Eqn 17	9.448e-5	0.9609	0.000129	-137.1	6

Table 2. Model statistics for θ_y

Info. measure	Model	Statistics				
		Standard error	R-squared	P-value	AICc	Degree of freedom
	Eqn 19	0.01194	0.2048	0.4483	-47.7	7
MI	Eqn 20	0.012	0.1974	0.4633	-63.7	7
	Eqn 21	0.01303	0.3242	0.6797	-25.4	5
	Eqn 22	0.002259	0.9857	3.49e-07	-81.0	7
Q_r	Eqn 23	0.0002907	0.9998	1.827e-11	-114.6	6
	Eqn 24	0.0003714	0.9996	1.136e-12	-117.2	7

Table 3. Model statistics for θ_z

Info. measure	Model	Statistics				
		Standard error	R-squared	P-value	AICc	Degree of freedom
	Eqn 25	0.012	0.3386	0.2353	-47.6	7
MI	Eqn 26	0.009741	0.6886	0.1473	-31.2	5
	Eqn 27	0.009918	0.7418	0.2202	-3.1	4
	Eqn 28	0.0006862	0.2779	0.32	-104.9	7
Q_r	Eqn 29	0.0007074	0.2325	0.396	-113.3	7
	Eqn 30	0.0005309	0.6294	0.0945	-102.5	6

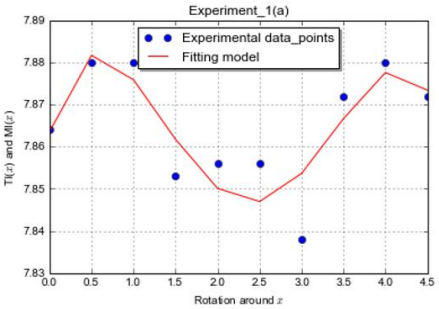

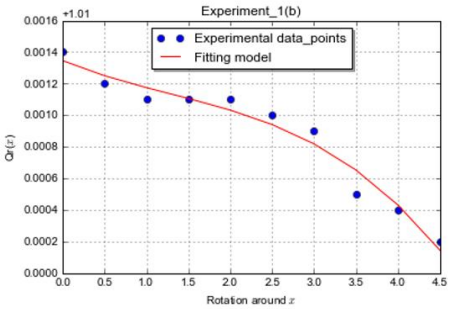

Fig. 4(a) **(b)**

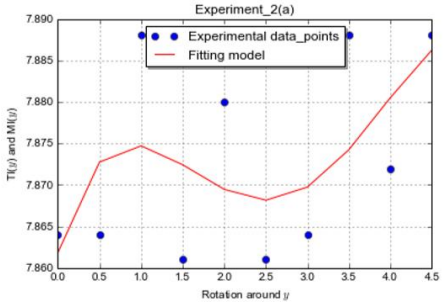

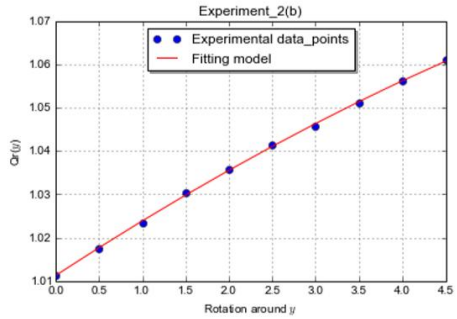

Fig. 5(a) **(b)**

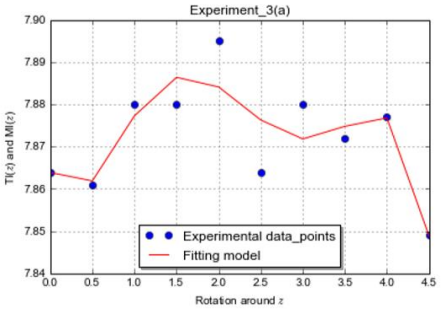

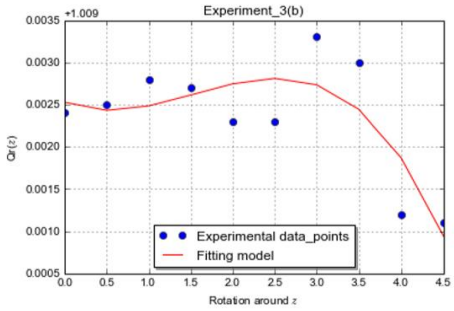

Fig. 6(a) **(b)**

Fig. 4a, 5a and 6a are plots of the information measure (mutual information) score experimentally measured at a contrast level of 50 while varying the image offset along θ_x, θ_y and θ_z respectively, combined with the polynomial model that fit the data distribution. Fig. 4b, 5b and 6b are the plot of the information measure (entropy quotient) score experimentally measured at a contrast level of 50 while varying the image offset along θ_x, θ_y and θ_z respectively, combined with the polynomial model that fit the data distribution

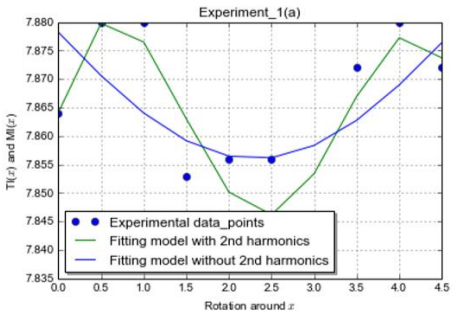

Fig. 7(a)

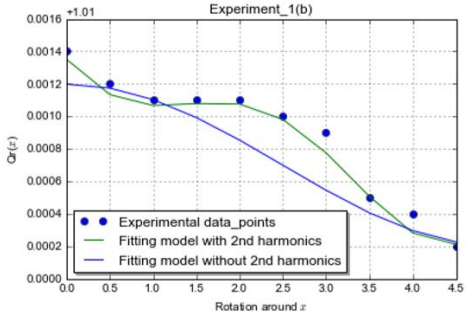

(b)

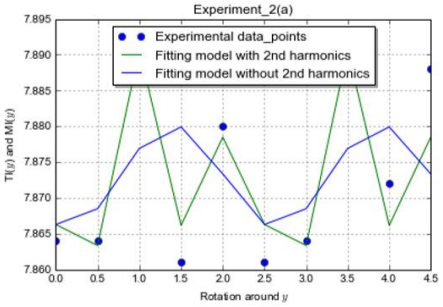

Fig. 8(a)

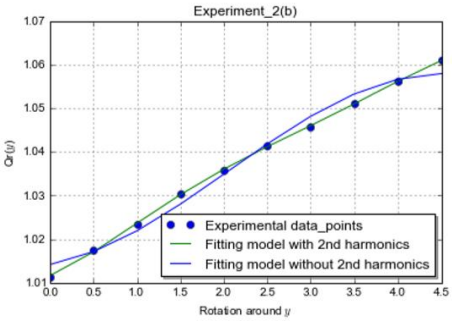

(b)

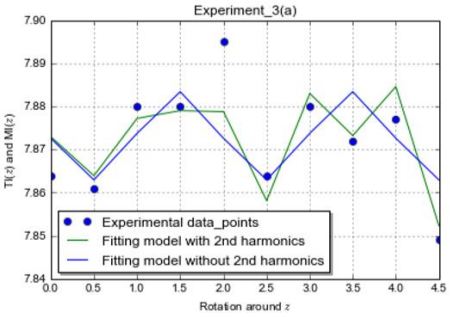

Fig. 9(a)

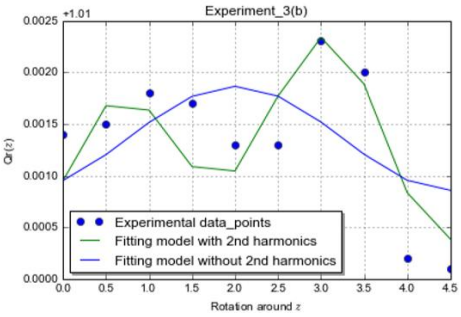

(b)

Fig. 7a, 8a and 9a are the plot of the information measure (mutual information) score experimentally measured at a contrast level of 50 while varying the image offset along θ_x, θ_y and θ_z respectively, combined with the first harmonic and second harmonic models that fit the data distribution. Fig. 7b, 8b and 9b are the plot of the information measure (entropy quotient) score experimentally measured at a contrast level of 50 while varying the image offset along θ_x, θ_y and θ_z respectively, combined with the first harmonic and second harmonic models that fit the data distribution

Table 4. Model statistics for translation along x

Info. measure	Model	Statistics				
		Standard error	R-squared	P-value	AICc	Degree of freedom
MI	Eqn 31	0.008212	0.2047	0.4487	-55.2	7
	Eqn 32	0.006826	0.6075	0.2935	-38.3	5
	Eqn 33	0.006176	0.6788	0.1577	-40.3	5
Q_r	Eqn 34	0.0001275	0.1934	0.4714	-138.5	7
	Eqn 35	0.0001313	0.1447	0.5786	-143.2	7
	Eqn 36	0.0001338	0.2383	0.6242	-130.1	6

Table 5. Model statistics for translation along y

Info. measure	Model	Statistics				
		Standard error	R-squared	P-value	AICc	Degree of freedom
MI	Eqn 37	0.01566	0.1238	0.6297	-42.3	7
	Eqn 38	0.0131	0.5621	0.3052	-25.3	5
	Eqn 39	0.01411	0.3897	0.3641	-36.9	6
Q_r	Eqn 40	0.000882	0.7223	0.01129	-99.9	7
	Eqn 41	0.0004515	0.948	0.002076	-92.6	5
	Eqn 42	0.0004508	0.9275	0.0001028	-113.3	7

Table 6. Model statistics for translation along z

Info. measure	Model	Statistics				
		Standard error	R-squared	P-value	AICc	Degree of freedom
MI	Eqn 43	0.009308	0.2358	0.3902	-52.7	7
	Eqn 44	0.009466	0.4355	0.5001	-31.8	5
	Eqn 45	0.009348	0.5595	0.508	-4.2	4
Q_r	Eqn46	0.00207	0.6112	0.03663	-82.8	7
	Eqn 47	0.0001761	0.7989	0.05433	-65.4	5
	Eqn 48	0.0002678	0.9935	2.226e-8	-123.6	7

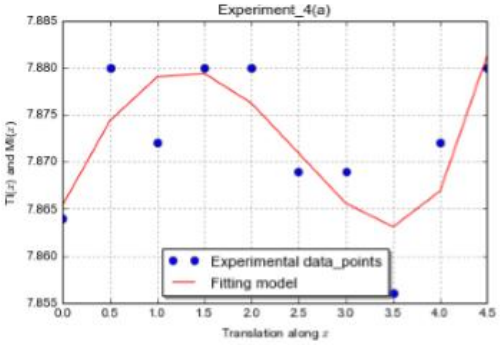

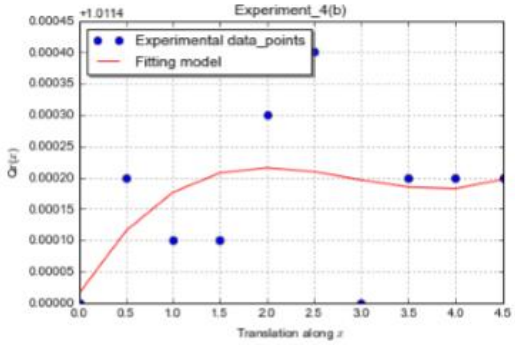

Fig. 10(a) **(b)**

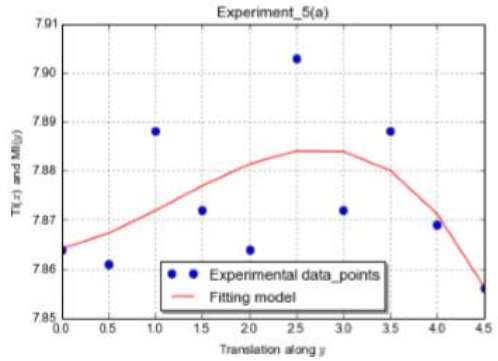

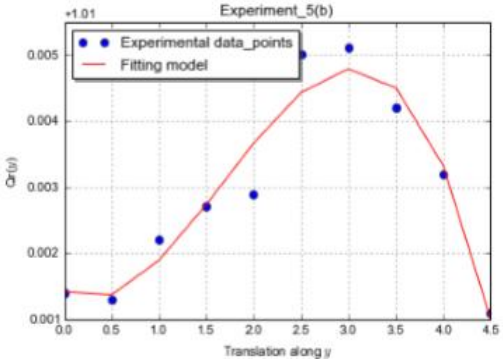

Fig. 11(a) **(b)**

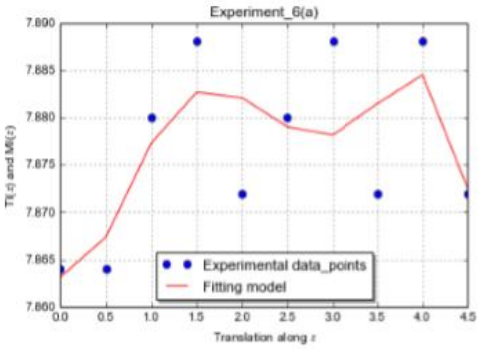

Fig. 12(a)

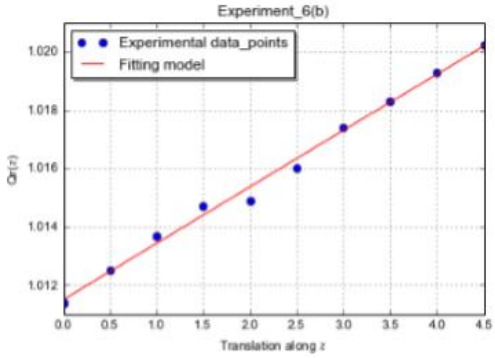

(b)

Fig. 10a, 11a and 12a are plots of the information measure (mutual information) score experimentally measured at a contrast level of 50 while varying the image offset along x, y and z respectively, combined with the polynomial model that fit the data. Fig. 10b, 11b and 12b are the plot of the information measure (entropy quotient) score experimentally measured at a contrast level of 50 while varying the image offset along x, y and z respectively, combined with the polynomial model that fit the data

7.3 Influence of Contrast on Similarity Measure

Before the choice of models, series of experiments were carried out on DRRs generated with various contrast level for a single patient. This was done with the interest of identifying how contrast change influences similarity measures. The result of the experiment is presented in form of graphs shown in Fig. 16.

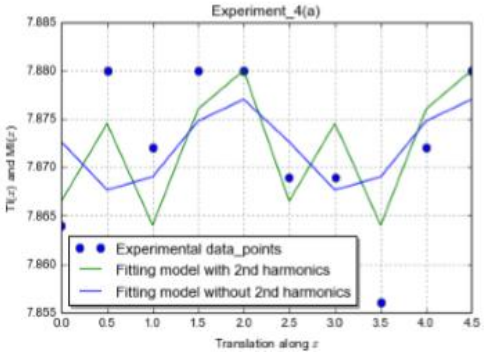

Fig. 13(a)

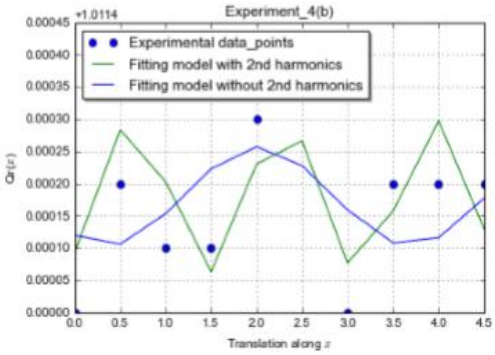

(b)

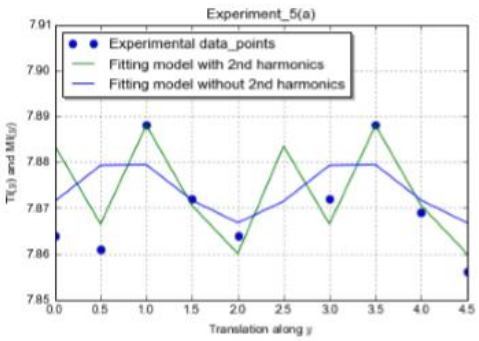

Fig. 14(a)

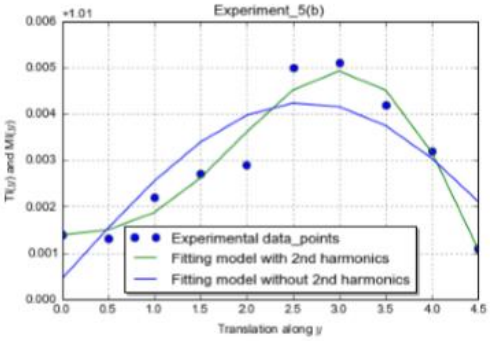

(b)

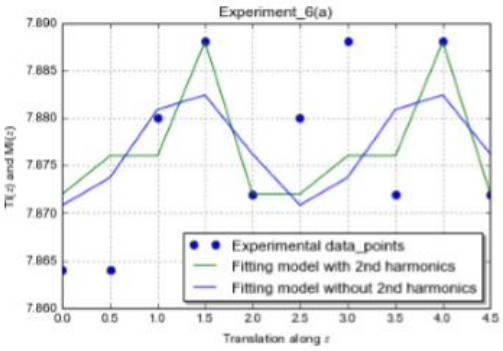

Fig. 15(a)

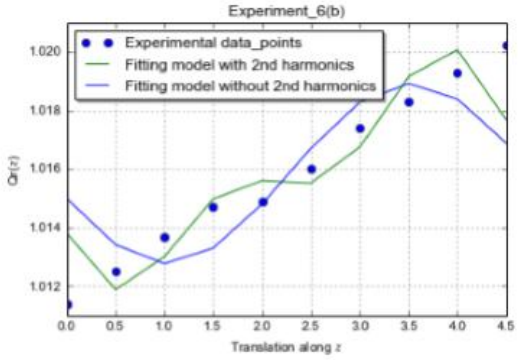

(b)

Fig. 13a, 14a and 15a are the plot of the information measure (mutual information) score experimentally measured at a contrast level of 50 while varying the image offset along x, y and z respectively, combined with the first harmonic and second harmonic models that fit the data. Fig. 13b, 14b and 15b are the plot of the information measure (entropy quotient) score experimentally measured at a contrast level of 50 while varying the image offset along x, y and z respectively, combined with the first harmonic and second harmonic models that fit the data.

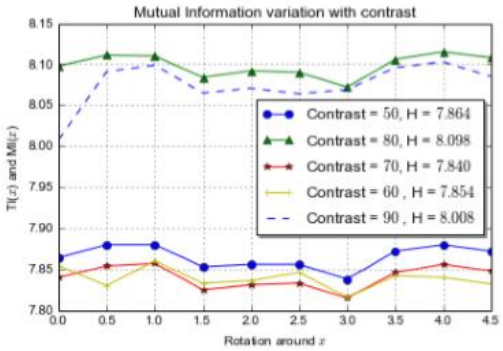

Fig. 16(a)

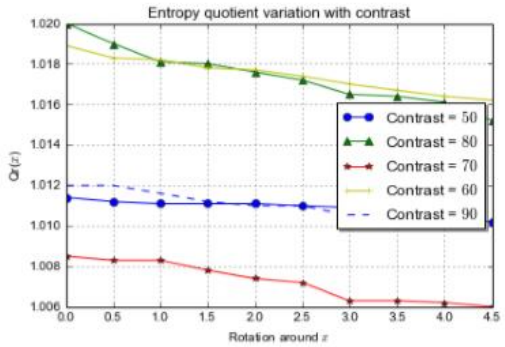

(b)

Fig. 16. Information measure variation with contrast for θ_x. (a) MI variation with contrast (b) Q_r variation with contrast

7.4 Model Testing

In general, a good regression model is the one that succeed in making the smallest possible errors while predicting the outcome of an experiment. We put some of the proposed model to test on another patient. The test was designed to evaluate the error that few of the proposed models make while predicting registration performance on another patient. The results of the tests are shown in Fig. 17.

The standard deviation between the experimental data and equation (24) shown in Fig. 17a is 0.0149 and for equation (32) shown in Fig. 17b is 0.0109. We choose these two models randomly from the set of screened models.

8. DISCUSSION

From Table 1, we observed that the prediction performance of equation (12) is the best among the three proposed models in the mutual information (MI) category, owing to its AICc score of −45.7. Furthermore, we observed that in the entropy quotient (Qr) category, equation (16) has the smallest AICc score of −147.0 which make it the best predicting model for the category. Comparing models representing both categories, we conclude that equation (16) with a standard

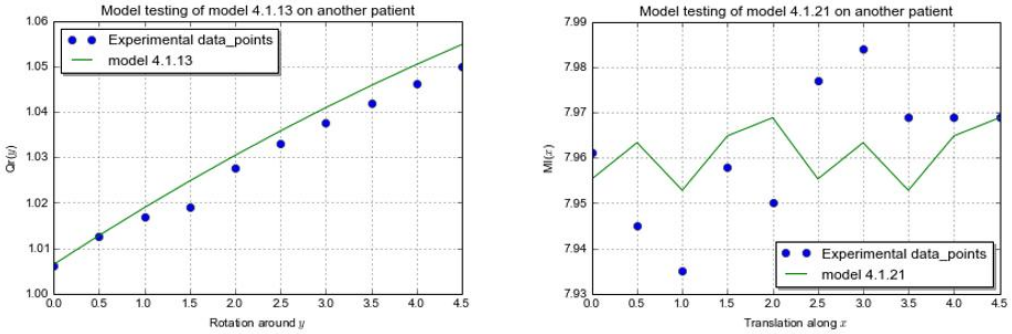

Fig. 17(a) **(b)**

Fig. 17. Result of performance test of proposed models on another patient. (a) equation (23) on another patient (b) equation (32) on another patient

error of 5.765×10−5 is the best model for predicting image registration performance of the system. Equation (16) has the ability to explain upto 98.54% of the effect of rotation offset around x by θ_x on the performance of registration output, should it be carried out. Therefore, we propose that the model given by equation (16) be used for prediction. Similarly, from Table 2, model given by equation (20) perform best after scoring an AICc mark of −63.7 in the MI category. Also, model given by equation (24) perform best in the Qr category with AICc score of −117.2. Comparing equation (20) and (24), based on their standard error and R-squared value, we can conclude that model given by equation (24) is the best for having the least standard error of 0.0003714. Equation (24) has the ability to explain upto 99.96% of the effect of rotating around y by θ_y on the performance of registration output, should it be carried out. Therefore, we propose that the model given by equation (24) be used for prediction. Furthermore, from Table 3, equation (25) perform best after scoring an AICc mark of −47.6 in the MI category. Also, equation (29) perform best in the Qr category with AICc score of −113.3. Comparing models in equations (25) and (29), based on their standard error and R-squared value, we can conclude that equation (29) is the best for having the least standard error of 0.0007074. However, equation (29) can only explain upto 23.23% of the effect of rotating around z by $\theta_z$on the performance of registration output, should it be carried out. Therefore, we propose that, though model in equation (30) has the highest AICc score (which is relatively low compared with all the models in the MI category and with standard error that is relatively low as well) in its category, however, since it can explain upto 62.94% of the effect of rotating around z by θ_z on the performance of registration output, it should be used for prediction.

On the variation of translation with contrast, from Table 4, we observed that the prediction performance of model in equation (31) is the best among the three proposed models in the mutual information (MI) category, owing to its AICc score of −55.2. Furthermore, we observed that in the entropy quotient (Qr) category, model in equation (35) has the least AICc score of −143.2 which make it the best predicting model for the category. Comparing models representing both categories (using their standard error and R-squared value), we may want to conclude that equation (35) with a standard error of 0.0001313 is the best model for predicting image registration performance of the system. However, the model has the ability to explain only upto 14.47% of the effect of translating along x on the performance of registration output, should it be carried out. Therefore, we propose that, though model in equation(32) has a high AICc score (but with standard error that is relatively low compared to model in equation (31)) in its category, however, since it can explain upto 67.88% of the effect of translating along x on the performance of registration output, it should be used for prediction. Similarly, from Table 5, model in equation (37) perform best after scoring an AICc mark of −42.3 in the MI category. Also, model in equation (42) perform best in the Qr category with AICc score of −113.3. Comparing equations (37) and (42), based on their standard error and R-squared value, we conclude that model in equation (42) is the best for having the least standard error of 0.0004508. Model in equation (42) has the ability to explain upto 92.75% of the effect of translating along y on the performance of registration output, should it be carried out.

Therefore, we propose that equation (42) be used for prediction. Lastly, from Table 6, model in equation (43) perform best after scoring an AICc mark of −52.7 in the MI category. Also, model in equation (48) perform best in the Qr category with AICc score of −123.7. Comparing equations (43) and (48), based on their standard error and R-squared value, we conclude that model in equation (48) is the best for having the least standard error of 0.0002678. Model in equation (48) have the ability to explain upto 99.35% of the effect of translating along z on the performance of registration output, should it be carried out. Therefore, we propose that it be used for prediction.

For the purpose of interest, it was also observed from figure (16) that the influence of contrast change on image registration performance is contained in the value of the intercepts of each models. This implies that the contrast change either increases or decreases the information entropy of an image. We therefore submit that the contrast change does not influence the pattern of distribution of information measure during registration, but provide an overall offset in response to change in information entropy of the reference image. Finally, from figure 17a and figure 17b which shows the performances of two of the proposed models – equation (24) and (32) respectively, it is obvious that the model performs very well. The degree of this performance is contained in their standard deviation. Equation (24) can predict the performance of registering radiograph from another patient using the entropy quotient Qr with a standard deviation of 0.0149. Equation (32) predicts registration performance on another patient using mutual information with a standard deviation of 0.0109. This is an interesting result that shows that indeed the proposed models predict image registration performance with high confidence and small error window.

9. CONCLUSION

We have experimentally studied image registration performance on posterior scans and have presented models that can be used to predict the registration performance of this type of scan relative to the source of misalignment or corruption as the case may be. Existing systems of performance evaluation in literature depend on post-processing data, which require expending computational energy before deciding whether or not the outcome of the exercise has achieved the purpose for which it was intended. In this work, we have been able to design a method to interpret information measures, such as the mutual information and entropy quotient, with the view of making decision on the need for registration. We have also presented models that help to predict performance of the same system before it is used, thereby saving us the computational cost of processing images. Meanwhile, we will like, in the future to look at possible extension of the present models to capture the effect of a simultaneous misalignment along or around two or more axes.

ACKNOWLEDGEMENT

The author will like to acknowledge the African Institute for Mathematical Sciences (AIMS) for the bursary awarded which enable this work to be carried out in the Republic of South Africa and Dr. Neil Muller for various suggestions when this work was on-going and for providing access to iThemba LABS DRR generation and Registration program and other data. The author also thanks Dr. Yansun Yao of the Physics and Engineering Physics Department of the University of Saskatchewan, Canada and anonymous reviewers for their constructive comments. Finally, the author acknowledges the travel grant from AIMS under the POST-AIMS bursary programme which enabled the completion of this research work.

COMPETING INTERESTS

Author has declared that no competing interests exist.

REFERENCES

1. Brown BH, Smallwood R, Barber D, Lawford P, Hose D. Medical physics and biomedical engineering. CRC Press; 1998.
2. Adeleke AA. Analytical solution to fundamental Bloch NMR flow equations for non-zero porosity transformation parameter. International Journal of Theoretical and Mathematical Physics. 2016;6(2):86-91.
DOI: 10.5923/j.ijtmp.20160602.04
3. Adeleke AA. Formulation of time dependent Bloch NMR equations for computational analysis of nanoparticles in porous media. British Journal of Mathematics and Computer Science. 2016;17(1):1-26.
DOI: 10.9734/BJMCS/2016/26359

4. Diamant E. Searching for image information content, its discovery, extraction, and representation. Journal of Electronic Imaging. 2005;14(1):013016–013016.
5. Gabarda S, Crist´obal G. No-reference image quality assessment through the von Mises distribution. J. of Optical Society of America – America. 2012;29(10):2058–2066.
6. Oliveira FP, Tavares JMR. Medical image registration: A review. Computer Methods in Biomechanics and Biomedical Engineering. 2014;17(2):73-93.
7. Wyawahare MV, Patil PM, Abhyankar HK, et al. Image registration techniques: An overview. International Journal of Signal Processing, Image Processing and Pattern Recognition. 2009;2(3):11-28.
8. Gonzalez RC, Woods RE. Digital Image Processing, 2nd. SL: Prentice Hall. 2002;2.
9. Bovik AC. The essential guide to image processing. Academic Press; 2009.
10. Roche A, Malandain G, Pennec X, Ayache N, et al. The correlation ratio as a new similarity measure for multimodal image registration. Medical Image Computing and Computer-Assisted Interventation—MICCAI'98. 1998;1115-1124.
11. Kashef BG, Sawetauk AA. A survey of new techniques for image registration and mapping. 27th Annual Techincal Symposium of International Society for Optics and Photonics ISOP. 1984;222–239.
12. Antoine Maintz MAVJB. Overview of medical image registration methods. Medical Imaging. IEEE Transactions. 2009;12(1):1-21.
13. Xie H, Hicks N, Keller GR, Huang H, Kreinovich V, et al. An interactive data language (IDL) /excelis visual information (ENVI) implementation of the fast fouriertransfrom-based algorithm for automatic image registration. Computers & Geosciences. 2003;29(8):1045-1055.
14. Brown LG. A survey of image registration techniques. Association of Computing Machinery (ACM) Computing Surveys (CSUR). 1992;24(4):325-376.
15. Cover TM, Thomas JA. Elements of information theory. John Wiley & Sons; 2006.
16. Vazquez-Fernandez E, Dacal-Nieto A, Martin F, Torres-Guijarro S, et al. Entropy of Gabor filtering for image quality assessment. Image Analysis and Recognition, Springer. 2010;52–61.
17. Daugman JG. Uncertainty relation for resolution in space, spatial frequency, and orientation optimized by two-dimensional visual cortical filters. J. Optical Society of America A. 1985;2(7):1160-1169.
18. Tsai D-Y, Lee Y, Matsuyama E. Information entropy measure for evaluation of image quality. Journal of Digital Imaging. 2008;21(3):338-347.
19. iThemba LABs digital head X-ray imaging system.
20. Carstens JE. Fast generation of digitally reconstructed radiographs for use in 2D-3D image registration. MSc. Thesis, University of Stellenbosch; 2008.
21. iThemba LABs Digitally Reconstructed radiograph (DRR) system.
22. Soong TT. Fundamentals of probability and statistics for engineers. John Wiley & Sons; 2004.
23. Dorfman DD, Alf E. Maximum-likelihood estimation of parameters of signal-detection theory and determination of confidence intervals - rating-method data. Journal of Mathematical Psychology. 1969;6(3):487-496.
24. Kendall Maurice G, Alan Stuart. Distribution theory. Charles Griffin; 1977.
25. Dorfman DD, Alf E. Maximum-likelihood estimation of parameters of signal-detection theory and determination of confidence intervals—rating-method data. Journal of Mathematical Psychology. 1969;6(3):487–496.
26. Bozdogan H. Model selection and akaike's information criterion (AIC): The general theory and its analytical extensions. Psychometrika. 1987;52(3):345-370.

Peer-review history:
The peer review history for this paper can be accessed here:
http://sciencedomain.org/review-history/16066